Kinetic Simulations of Instabilities in Cylindrical Magnetized Jets

José Ortuño-Macías[1] and Krzysztof Nalewajko[1]

1. Nicolaus Copernicus Astronomical Center, Polish Academy of Sciences, Bartycka 18, 00–716 Warszawa, Poland; jortuno@camk.edu.pl

High-energy astrophysical phenomena commonly involve regions with magnetic energy density that locally dominates the rest-mass energy density of matter. Such relativistic magnetizations can be converted to relativistic particle acceleration, which is observed in the form of luminous non-thermal emission with photon energies extending into the gamma-ray band. Relativistically magnetized regions are expected in the relativistic jets, which may involve ordered magnetic fields with poloidal and toroidal components, the latter prone to the $m = 0$ pinch and $m = 1$ kink instability modes (Begelman, 1998). Recently, the first 3D kinetic numerical simulations of cylindrical magnetized columns reported efficient particle acceleration in two different magnetic field configurations, with the toroidal field supported either by the poloidal field (Davelaar et al., 2020) or by the gas pressure (Alves et al., 2018). Here we report preliminary results from our 3D kinetic simlations of cylindrical magnetized columns with the toroidal field supported by a combination of poloidal field and gas pressure.

1 Initial Configuration

We used a modified version of the publicly available particle-in-cell (PIC) code `Zeltron` (Cerutti et al., 2013). We fit axisymmetric equilibria of outer radii $R_{\rm out} = L/2$, centered along the axis $x = y = L/2$, where L is the physical size of the computational domain. The equilibrium is based on the radial profile of toroidal magnetic field $B_\phi(r)$ in the form of a power-law with inner and outer cutoffs (see Fig. 1):

$$B_\phi(r) = B_0 \left(\frac{r}{R_0}\right)^{\alpha_{\rm B\phi}} C(s_{\rm B\phi}, r)\, C(s_{\rm B\phi}, R_{\rm out} - r), \tag{1}$$

where $C(s_{\rm B\phi}, r) = (r/R_0)^{s_{\rm B\phi}}/[1 + (r/R_0)^{s_{\rm B\phi}}]$ with parameters $\alpha_{\rm B\phi} \leq 0$, $s_{\rm B\phi} = 1 - \alpha_{\rm B\phi}$, the core radius $R_0 = R_{\rm out}/10 = L/20$. The initial equilibrium is provided by the electric current $j_{\rm z(r)} = (c/4\pi r)\mathrm{d}(rB_\phi)/\mathrm{d}r$, as well as by the combination of poloidal magnetic field $B_z(r)$ and gas pressure $P(r)$. We introduce a constant parameter $f_{\rm mix} \in [0:1]$, which is the fraction of toroidal magnetic stress supported by the gas pressure gradient (with the remainder supported by the poloidal magnetic pressure):

$$\frac{\mathrm{d}P}{\mathrm{d}r} = -f_{\rm mix}\frac{B_\phi}{4\pi r}\frac{\mathrm{d}(rB_\phi)}{\mathrm{d}r}, \tag{2}$$

$$\frac{\mathrm{d}B_{\rm z}^2}{\mathrm{d}r} = -(1 - f_{\rm mix})\frac{2B_\phi}{r}\frac{\mathrm{d}(rB_\phi)}{\mathrm{d}r}, \tag{3}$$

with the initial density profile $n(r) = P(r)/\Theta_0 m_{\rm e}c^2$, where $\Theta_0 = kT_0/m_{\rm e}c^2$. In addition, we have investigated different density ratios $\xi_{\rm n} \equiv n_{\rm max}/n_{\rm min}$, where $n_{\rm min/max}$

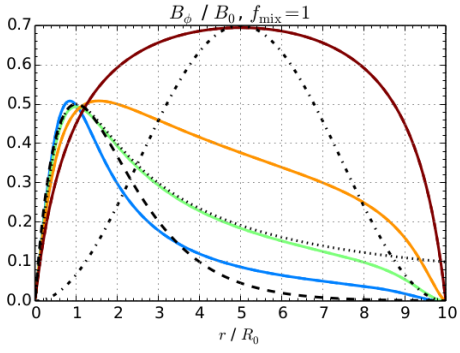

Fig. 1: Radial profiles of the initial toroidal field $B_\phi(r)$ profiles in units of B_0 compared for $\alpha_{\rm B\phi} = 0, -0.5, -1, -1.5$. We also show the $B_\phi(r)$ profiles of Davelaar et al. (2020) and Alves et al. (2018) in black dotted and dash lines, respectively.

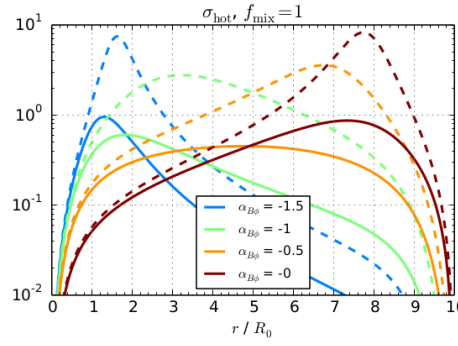

Fig. 2: Radial profiles of the initial magnetization parameter. Solid lines correspond to a moderate density ratio $\xi_{\rm n} = 10$, and dashed lines correspond to a high density ratio $\xi_{\rm n} = 100$.

are the extreme values of $n(r)$. A higher density ratio results in a higher initial magnetization $\sigma = B_0^2/4\pi\Theta_0 n m_{\rm e} c^2$ (see Fig. 2).

2 Selected Results

- In our reference case for $\alpha_{\rm B\phi} = -1$ and $f_{\rm mix} = 1$, we find a well defined fast magnetic dissipation phase for $1.0 < ct/L < 1.6$ (Fig. 3), corresponding to a rapid decrease of the toroidal magnetic flux $\Psi_{\rm B\phi}$ (thick solid green line), a strong spike of the axial electric field $E_{\rm z}$ (solid magenta line), and a rapid increase of $\gamma_{\rm max}$ (solid red line) to the level comparable with the particle energy limit $\gamma_{\rm lim}$ identified by Alves et al. (2018). However, the $\gamma_{\rm lim}$ energy limit is strongly exceeded in the cases of $\alpha_{\rm B\phi} < -1$ due to the extended duration of the fast magnetic dissipation phase.
- In our simulations particle acceleration is dominated by ideal electric fields perpendicular to their local magnetic fields. However, acceleration by parallel electric fields was previously reported in the $f_{\rm mix} = 0$ limit by Davelaar et al. (2020). Fig. 4 shows the fractions of total energy gains δ_γ that can be attributed to the perpendicular electric fields $\delta_{\gamma\perp}$. During the most efficient particle acceleration these fractions achieve the level of $\sim 85-90\%$, which does not depend on the value of $f_{\rm mix}$.
- The $m = 0$ pinch and $m = 1$ kink instability modes saturate at a later time and show a slower growth for a higher value of $\alpha_{\rm B\phi}$ and a lower value of $f_{\rm mix}$. The onsets of the pinch mode are delayed with respect to the onsets of the kink mode. Both modes appear to originate in the central core ($r < R_0$), and they propagate outwards with similar speeds.

Acknowledgements. This is a preliminary report of our results that will be submitted for publication in collaboration with Dmitri A. Uzdensky, Mitchell C. Begelman, Alex Chen,

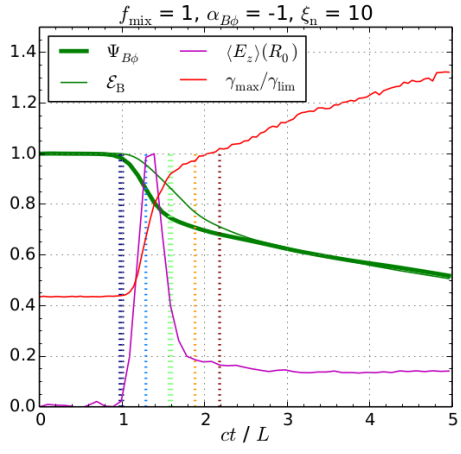

Fig. 3: Time evolution of the total magnetic field (thin green line), toroidal magnetic flux (thick green line), mean axial electric field averaged over z an ϕ at $r = R_0$ (magenta line) and maximum particle energy $\gamma_{\rm max}$ normalized to $\gamma_{\rm lim}$; for the gas pressured supported case with $\alpha_{\rm B\phi} = -1$.

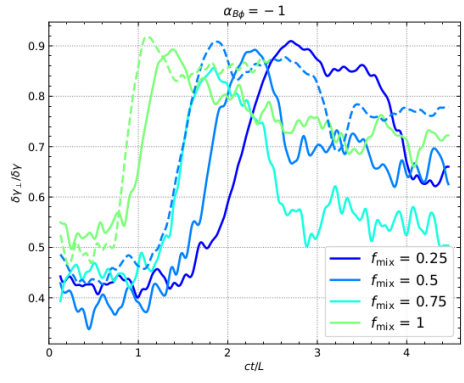

Fig. 4: Relative contribution of perpendicular electric fields (ideal MHD electric field) to the positive energy gains of energetic particles as function of simulation time for simulations with $\alpha_{\rm B\phi} = -1$.

Gregory Werner and Bhupendra Mishra. Simulations were performed at the supercomputer `Prometheus` located at the Academic Computer Centre 'Cyfronet' of the AGH University of Science and Technology in Krakow, Poland (PLGrid grants `pic19, plgpic20, ehtsim`). This work is supported by the Polish National Science Centre grant 2015/18/E/ST9/00580.

References

Alves, E. P., Zrake, J., Fiuza, F., *Phys. Rev. Lett.* **121**, 24, 245101 (2018)

Begelman, M. C., *ApJ* **493**, 1, 291 (1998)

Cerutti, B., Werner, G. R., Uzdensky, D. A., Begelman, M. C., *ApJ* **770**, 2, 147 (2013)

Davelaar, J., Philippov, A. A., Bromberg, O., Singh, C. B., *ApJL* **896**, 2, L31 (2020)